Pergamon

Int. J. Heat Mass Transfer. Vol. 39, No. 13, pp. 2711–2722, 1996

0017-9310/96 $15.00+0.00

0017-9310(95)00362-2

Heat transfer in a pressurized circulating fluidized bed

PRABIR BASU and LEMING CHENG†

Department of Mechanical Engineering, Technical University of Nova Scotia, Halifax, Nova Scotia, B3J 2X4 Canada

and

KEFA CEN

Department of Energy Engineering, Zhejiang University, Hangzhou, Zhejiang, 310027, People's Republic of China

(*Received* 14 *April* 1995 *and in final form* 22 *September* 1995)

Abstract—Bed-to-wall heat transfer in a pressurized circulating fluidized bed is analyzed. The cluster renewal model is modified to account for the effect of pressure on heat transfer. Bed-to-wall heat transfer coefficients at different operating pressures were measured. The effects of system pressure, bed suspension density, particle size and superficial gas velocity were investigated in the tests. In addition to the modified model, a semi-empirical equation based on the test data is proposed for the prediction of heat transfer coefficients. A comparison with experimental data in the literature, as well as those from the present work, shows a good agreement. Copyright © 1996 Elsevier Science Ltd.

INTRODUCTION

Pressurized fluidized beds are beginning to be used for power generation. This type of plant benefits from a number of special features of pressurized fluidized bed combustion technology [1]: (1) improved plant efficiency (lower heat rate); (2) reduced emissions and improved combustion; (3) reduced boiler size; (4) reduced tube wastage; (5) modularity.

There are two types of pressurized fluidized beds: bubbling and circulating. While pressurized bubbling-bed designs have been developed and are in commercial operations, the circulating fluidized bed (CFB) designs are still in the pilot stage. However, in order to fully comprehend the advantages of pressurized circulating fluidized beds (PCFBs) and to produce a realistic conceptual design, it is important to understand the effect of pressure on different design parameters. The bed-to-wall heat transfer coefficient is one of the important parameters whose knowledge is required during both the design and operating phase of a boiler. So an attempt has been made to study this aspect of PCFBs, both theoretically and experimentally. For the sake of scale up and parametric study, a mechanistic model is developed by extending an earlier model [2] for atmospheric pressure. Then on the basis of experiments conducted, an empirical relation is developed for the prediction of heat transfer coefficients, within the present range of experiments.

MODEL

A PCFB operates at several atmospheric pressures. Higher gas densities under higher system pressures may have a major bearing on the heat transfer coefficients. This model is an extension of the one developed by Basu [2] for atmospheric pressure CFB. Since the model is described in detail by Basu [2], only the improvements are indicated here.

The riser of a CFB operating under a fast fluidized regime comprises two phases: clusters and dispersed phase [3]. At any instant (Fig. 4), the wall of the bed is covered partially by clusters and partially by the dispersed phase. Thus the bed-to-wall convective heat transfer coefficient, h_{conv} would have two components: one due to the clusters h_c and the other due to the dispersed phase, h_d. The fraction of the wall covered by the clusters δ_c may be estimated as [2]

$$\delta_c = K\left[\frac{(1-\varepsilon_w - Y)}{(1-\varepsilon_c)}\right]^{0.5} \quad (1)$$

where $K = 0.5$, ε_w is the voidage near the wall, which can be obtained by $\varepsilon_w = \varepsilon(r_i = R) = \varepsilon^{3.811}$ [4], ε_c is the voidage within the clusters, Lints [5] derived the average solid concentration in the clusters at the wall

† On leave from Department of Energy Engineering, Zhejiang University, Hangzhou, 310027, People's Republic of China.

NOMENCLATURE

Ar $= d_p^3 \rho_g(\rho_p - \rho_g)g/\mu^2$, Archimedes number
C_c, C_g, C_p specific heat of cluster, gas and bed solids respectively [kJ kg^{-1} °C^{-1}]
D diameter of the bed [m]
d_i, d_o inside and outside diameter of the heat transfer section, respectively [m]
d_p diameter of average bed particles [m]
Expt experiment data
g acceleration due to gravity, 9.81 [m s^{-2}]
h heat transfer coefficient [kW m^{-2} °C^{-1}]
h_c convective heat transfer coefficient due to clusters [kW m^{-2} °C^{-1}]
h_{conv} bed-to-wall convective heat transfer coefficient [kW m^{-2} °C^{-1}]
h_d modified convective heat transfer coefficient due to dispersed phase [kW m^{-2} °C^{-1}]
K constant in equation (1)
K_c, K_g thermal conductivity of cluster and gas respectively [kW m^{-1} °C$-$1]
K_{gf}, K_p thermal conductivity of gas-film on the wall, solids, respectively [kW m^{-1} °C^{-1}]
K_s thermal conductivity of the heat transfer section [kW m^{-1} °C^{-1}]
L length [m]
Nu_w $= hd_p/K_g$, Nusselt number for bed-to-wall heat transfer
Nu_D $= hD/K_g$, Nusselt number of the bed,
Pr Prandtl number of gas
R radius or half-width of the bed [m]
r_i radial distance from the bed center [m]
Re_D $= DU_g\rho_g/\mu$, Reynolds number in the bed
Re_p $= d_pU_g\rho_g/\mu$, particle Reynolds number
T_b bed temperature [°C]
T_{wi}, T_{wo} inside and outside temperature of the heat transfer section [°C]
t time [s]
t_c average residence time of clusters on the wall [s]
U_g, U_m superficial gas velocity and maximum fall velocity of clusters [m s^{-1}]
U_{mf} superficial gas velocity at minimum fluidizing condition [m s^{-1}]
U_t terminal velocity of average size bed particle [m s^{-1}]
V_s solids velocity in the standpipe of loop-seal [m s^{-1}]
Y volume fraction of solid in the dispersed phase.

Greek symbols
δ_c time average fraction of wall area covered by clusters
ε, ε_c, ε_w bed cross-section average voidage, cluster voidage, voidage near the wall
μ viscosity of gas [kg m^{-1} s^{-1}]
ρ_0 density of gas at standard condition (0°C, 100 kPa) [kg m^{-3}]
ρ_c, ρ_{dis}, ρ_g density of cluster dispersed phase and gas respectively [kg m^{-3}]
ρ_{g0} density of gas at bed temperature under 100 kPa [kg m^{-3}]
ρ_p density of bed solids [kg m^{-3}].

$(1-\varepsilon_c)$ of the bed from the capacitance probe data of Wu *et al.* [6], Dou [7] and Louge *et al.* [8] as

$$1-\varepsilon_c = 1.23(1-\varepsilon)^{0.54} \quad (2)$$

where ε is the cross-section average voidage of solids. The volume fraction of solid in the dispersed phase Y may be taken as 0.001% [2, 3].

Thus the bed-to-wall convective heat transfer coefficient h_{conv} can be expressed as

$$h_{conv} = \delta_c h_c + (1-\delta_c)h_d. \quad (3)$$

The convective heat transfer coefficient due to the particles or clusters may be written as [2]

$$h_c = \frac{1}{\dfrac{d_p}{10K_{gf}} + \left(\dfrac{t_c\pi}{4K_cC_c\rho_c}\right)^{0.5}} \quad (4)$$

where d_p is the particle diameter, K_{gf} is the thermal conductivity of gas film evaluated at the mean gas-film temperature, t_c is the average residual time of clusters on the wall, which can be calculated referring to the literature [11]. K_c, C_c and ρ_c are the thermal conductivity, specific heat and density of the cluster, respectively. $C_c = [(1-\varepsilon_c)C_p + \varepsilon_cC_g]$ and $\rho_c = [(1-\varepsilon_c)\rho_p + \varepsilon_c\rho_g]$, respectively. The thermal conductivity of cluster, K_c, is taken from the following equation [9]:

$$K_c = K_g\left(\frac{K_p}{K_g}\right)^{[0.28-0.757\log 10\varepsilon c - 0.057\log 10(K_p/K_g)]} + 0.1\rho_gC_gd_pU_{mf}. \quad (5)$$

The gas thermal conductivity K_g may be assumed independent of pressure because it changes by less than 2% whereas the pressure changes from 100 kPa to 1000 kPa at the same bed temperature [Fig. 1(b)].

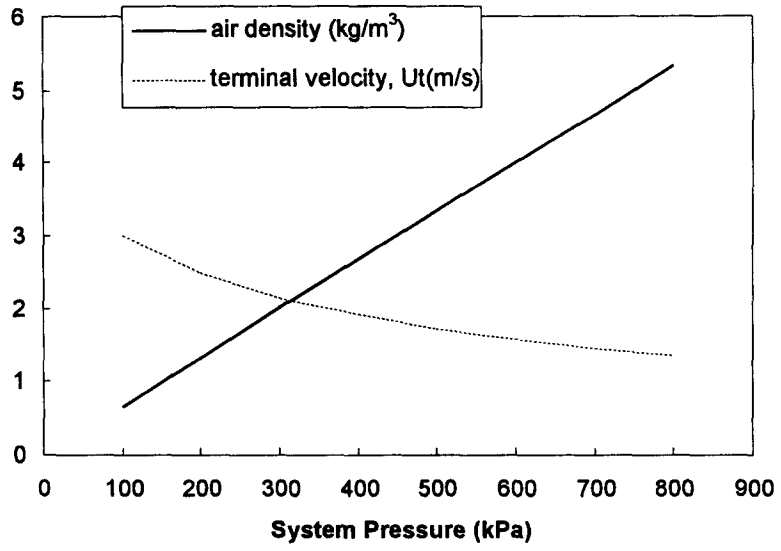

(a) density of air and particle terminal velocity

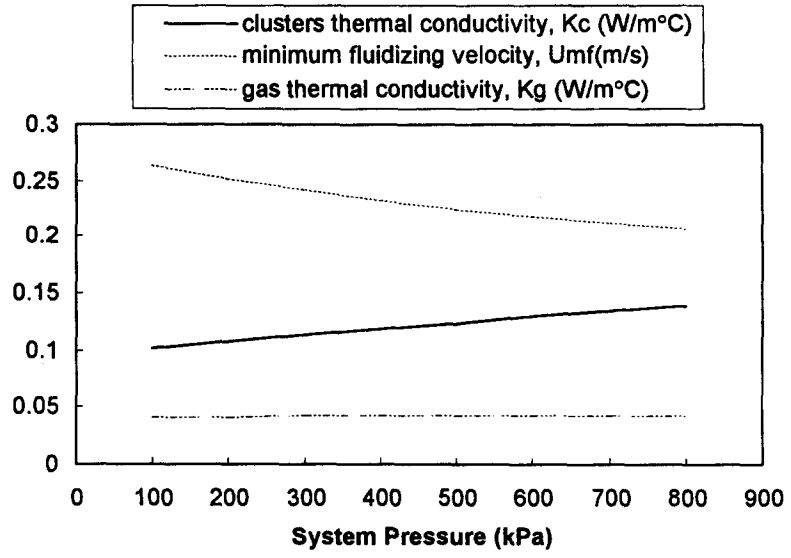

(b) thermal conductivity and minimum fluidizing velocity

Fig. 1. Parameters change under different system pressures, (a) density of air and particle terminal velocity, (b) thermal conductivity and minimum fluidizing velocity (calculation condition: bed temperature 250°C, suspension density 15 kg m^{-3}).

The minimum fluidization velocity U_{mf} may be predicted by the Ergun equation [10]. The maximum fall velocity of clusters U_m is taken as 1.26 m s^{-1} in the model calculation [3].

The convective heat transfer due to the upflowing dispersed phase as given by Basu [2] for atmospheric pressure could not reflect the effect of the pressure very well. Xavier and Davidson [9] and Martin [12] found that the gas convective heat transfer coefficient varies approximately as the square root of the gas density. So the Wen and Miller [13] equation used by Basu [2] was modified as

$$h_d = \frac{K_g}{d_p}\frac{C_p}{C_g}\left(\frac{\rho_{dis}}{\rho_p}\right)^{0.3}\left(\frac{U_t^2}{g d_p}\right)^{0.21} Pr\left(\frac{\rho_g}{\rho_{go}}\right)^{0.2} \quad (6)$$

where the density of dispersed phase $\rho_{dis} = \rho_p Y + \rho_g(1-Y)$, the terminal velocity of a particle

U_t is calculated by the equation presented by Haider and Levenspiel [14].

PARAMETRIC STUDY

The effect of pressure on the heat transfer being the major object of this work, the pressure dependence of different parameters is discussed below using the above model. Figure 1 (a, b) shows the computed variations of air density, particle terminal velocity U_t, cluster thermal conductivity and minimum fluidization velocity U_{mf} with changing system pressures. An increase in the pressure causes a proportional increase in the gas density [Fig. 1(a)], and an increase in the cluster thermal conductivity [Fig. 1(b)]. However, both particle terminal velocity U_t and minimum fluidizing velocity U_{mf} decrease [Fig. 1(a, b)] with pressure.

Figure 1(b) also plots the effect of pressure on the thermal conductivity of gas [15]. It shows that the thermal conductivity of gas decreases with the pressure, but only to a marginal extent. This suggests that the major influence of pressure on the heat transfer is due to the change in the gas density, rather than that in the cluster thermal conductivity.

The heat transfer coefficients are computed using equations (1)–(6). The computed heat transfer coefficients are plotted against the system pressure on Fig. 2. From here we note that: (1) the bed-to-wall heat transfer coefficient h_{conv} increases with increasing of gas density; (2) the effect of pressure on U_t and U_{mf} tends to reduce the convective heat transfer coefficient; however, at a higher pressure the U_t becomes less dependent on the pressure [Fig. 1(a)], and therefore, its effect on h_{conv} declines; (3) the thermal conductivity of the cluster, K_c, which increases with pressure, would try to increase the convective heat transfer coefficient, h_{conv}.

The combined influence of these parameters on the convective heat transfer coefficient is shown on Fig. 2. The bed-to-wall heat transfer coefficient h_{conv} clearly increases with an increase in the system pressure.

The effect of pressure predicted so far as based on the mechanistic model developed earlier. These predictions are accurate to the extent the model is. So, experiments were carried out in a PCFB to verify the above observations and to validate the model.

EXPERIMENTAL APPARATUS AND METHODS

Figure 3 shows a schematic of the PCFB test rig. The diameter and height of the fast fluidized bed are ϕ52.5 mm(ID) and 2020 mm, respectively. Most particles were separated in the primary cyclone and recycled to the bed through the standpipe and the loop-seal. The gas, separated in the cyclone, passed through a secondary cyclone and then went up a stack through an exit valve. The entire test rig is located in a temperature controlled electric furnace. The enclosing furnace wall is shown by a dotted line in Fig. 3. The fluidizing air was supplied by a compressed air source (700 kPa max.). The pressure in the bed was adjusted by controlling the exit valve. System pressures were read from pressure gauges located in the riser.

The bed suspension in the riser was determined from the measured pressure drop along the bed height. Two measuring devices were used to measure the pressure drop along the bed (1) a Durablock® Solid Plastic Stationary Gage; (2) a Model 700D5″24V4 Pressure Transducer. Considering the high pressure inside the bed, the pressure transducer was arranged in a pres-

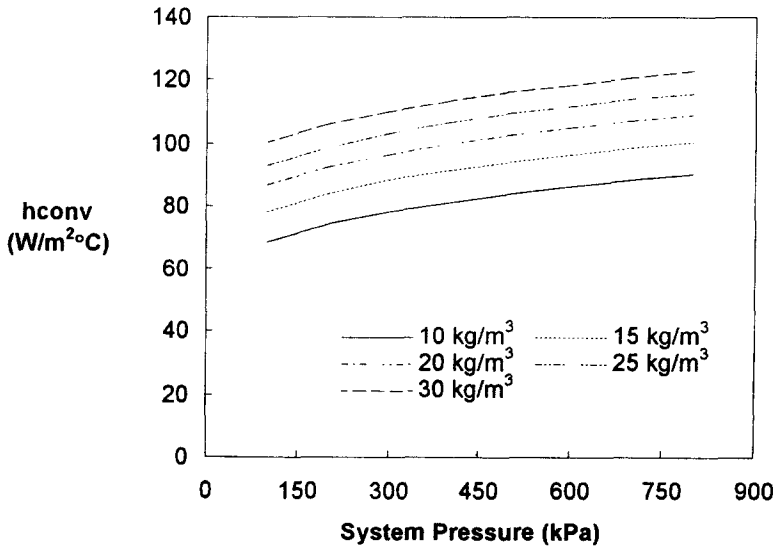

Fig. 2. Bed-to-wall convective heat transfer coefficients at different system pressures (calculation condition: bed temperature 250°C, suspension density 15 kg m^{-3}).

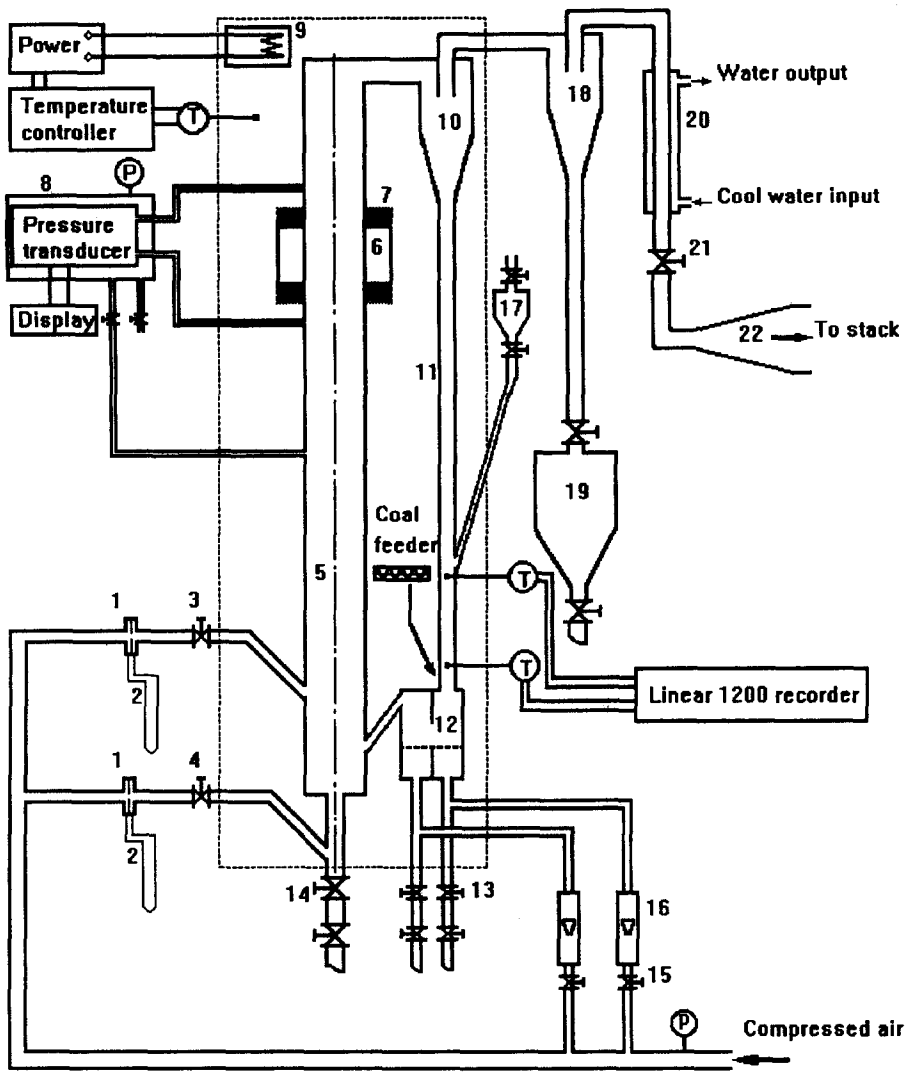

Fig. 3. System schematic of the pressurized circulating fluidized bed test rig.

sure vessel to minimize the pressure balance across the transducer wall (Fig. 3).

To measure the solid recycle rate in the tests, two K-type thermocouples were located at two elevations in the standpipe (Fig. 3). Cold sand is dropped from a tank (17 in Fig. 3). The sand moves together with the recycled solids as a plug in the standpipe. The arrival of the cold charge of sand at an elevation will be detected by a drop in temperature, marked by the thermocouple at that elevation. Electric signals from the thermocouples are recorded by a Linear 1200 Recorder. The solids velocity in the standpipe can then be calculated by

$$V_s = L/t \tag{7}$$

where L is the height separating two thermocouples and t is the time difference between the two occurrence of temperature drops.

Heat transfer section

A solid hollow cylindrical heat transfer section, made of stainless steel, was used to measure the heat

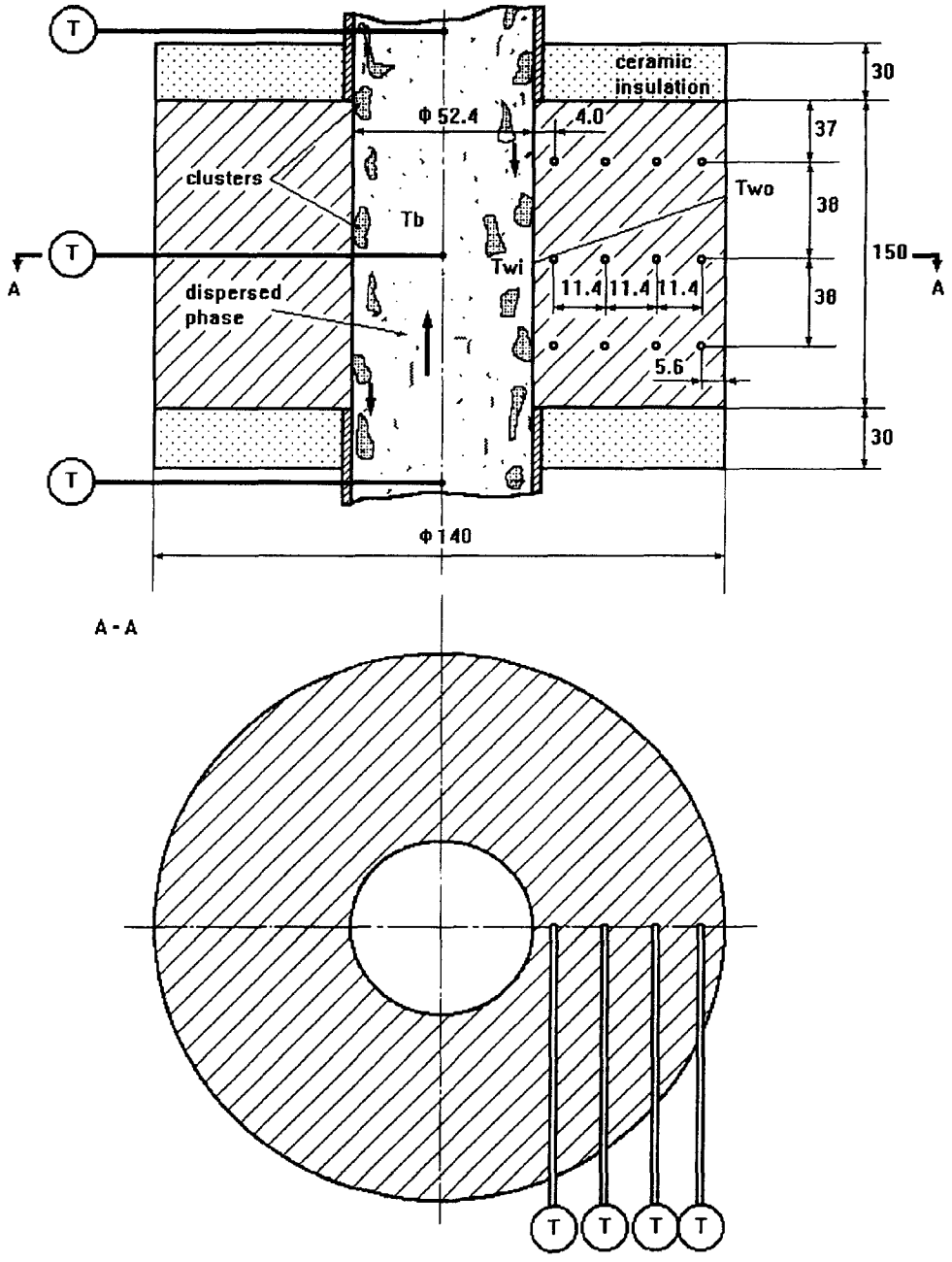

Fig. 4. Heat transfer section.

transfer coefficients (Fig. 4). Its inside diameter is the same as that of the bed column. The outside diameter is 140 mm and the height is 150 mm. Along the radial direction, 12 K-type thermocouples were inserted in the heat transfer section, at three levels. To reduce any heat loss along the vertical direction of the heat transfer section, a 30 mm layer of refractory ceramic fiber was provided on each side of the heat transfer section. Thus, heat loss from the top and bottom ends of the section can be neglected.

In the present test rig the enclosing furnace heats the bed, so heat is transferred from outside of the section into the bed. Neglecting heat losses from the section's top and bottom, the bed-to-wall heat transfer coefficients in the bed can be calculated according to the heat balance among the bed, heat transfer section and the surrounding

$$h = \frac{2K_s(T_{wo} - T_b)}{d_i(T_{wi} - T_b)\ln(d_0/d_i)}. \quad (8)$$

The temperatures of the inner and outer wall of the heat transfer section, T_{wi} and T_{wo}, were obtained from an extrapolation of the measured radial temperature

profile in the heat transfer section. T_b is the bed temperature.

To verify the accuracy of the above heat transfer measurement technique, only air was passed through the riser at atmosphere pressure and the forced convective heat transfer coefficient was measured. The measured value was compared with that computed from the well known Dittus–Boelter equation for forced convection in a pipe: $Nu_D = 0.023 Re_D^{0.8} Pr^{0.4}$. The difference was only 9.2%, which was acceptable.

Two types of sand particles were used in the tests. The arithmetic mean diameter of sand I is 0.507 mm, while that of sand II is 0.232 mm. The density, bulk density, minimum fluidizing velocity, terminal velocity and sphericity of sand I and II are 2818 kg m^{-3}, 1400 kg m^{-3}, 0.27 m s^{-1}, 2.56 m s^{-1}, 0.66 and 2730 kg m^{-3}, 1422 kg m^{-3}, 0.043 m s^{-1}, 1.29 m s^{-1} and 0.62, respectively. Both of these two sands belong to Group B in Geldart classification.

EXPERIMENTAL RESULTS AND DISCUSSION

Several factors would affect the bed-to-wall heat transfer coefficient in a PCFB. The effects of only the main operating parameters on the heat transfer coefficient were studied in this series of experiments. Heat transfer coefficients were measured by varying the system pressure (100 kPa–600 kPa), bed suspension density (8 kg m^{-3} ~ 35 kg m^{-3}), and solid particle (0.507 mm, 0.232 mm). The influence of superficial gas velocity was also studied in the range of 3.6 ~ 4.8 m s^{-1}.

Effect of system pressure

At a given pressure the bed suspension density was adjusted by controlling the solid recycle rate and the superficial gas velocity. Thus, the influence of system pressure on the heat transfer coefficient is obtained at similar suspension densities, which is shown on Fig. 5. The data show that the heat transfer coefficient increases as the system pressure increases. The increase in gas density with increasing pressure is the primary reason for enhancement of the convective heat transfer. The thermal conductivity of the clusters also increases with the pressure, contributing further to an improved thermal contact between the clusters and wall. Shen *et al.* [16] suggested that there is a tendency of shift from aggregative fluidization to dispersion fluidization with the increase in operating pressure. This may decrease the solid concentration near the wall. This suggestion should demonstrate an opposite effect of pressure on the heat transfer. A detailed measurement of solid concentrations near the wall at different pressures is necessary to resolve this question.

The operating conditions of this series of experiments were fed into the modified model. Predicted values are compared with those measured data (Fig. 5). An excellent agreement between measured data and predicted results is noted. This verifies the validity of the model for PCFB.

Effect of suspension density

The heat transfer coefficient in the PCFB increases with an increase in the suspension density. The test and model results are presented on Fig. 6 for different operating pressures. The heat transfer coefficient increased with suspension density in all cases. The variation in heat transfer coefficient with the suspension density is similar under all bed pressures (Fig. 6), even though the gas phase plays an increasingly

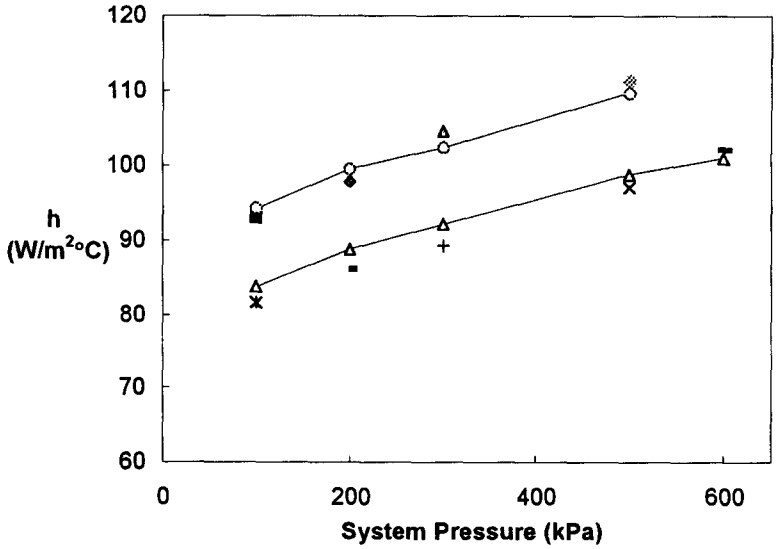

Fig. 5. Effect of system pressure on the heat transfer coefficients and the present model results (particle diameter: 0.507 mm). ■ 25.8 kg m^{-3}, 1.74 m s^{-1}, ◆ 25.4 kg m^{-3}, 1.94 m s^{-1}, ▲ 24.9 kg m^{-3}, 1.26 m s^{-1}, ● 25.2 kg m^{-3}, 1.55 m s^{-1}, * 17.6 kg m^{-3}, 4.57 m s^{-1}, – 17.5 kg m^{-3}, 3.15 m s^{-1}, + 17.1 kg m^{-3}, 3.77 m s^{-1}, × 17.7 kg m^{-3}, 2.93 m s^{-1}, — 17.8 kg m^{-3}, 1.15 m s^{-1}, ○ △ predicted values for corresponding parameters.

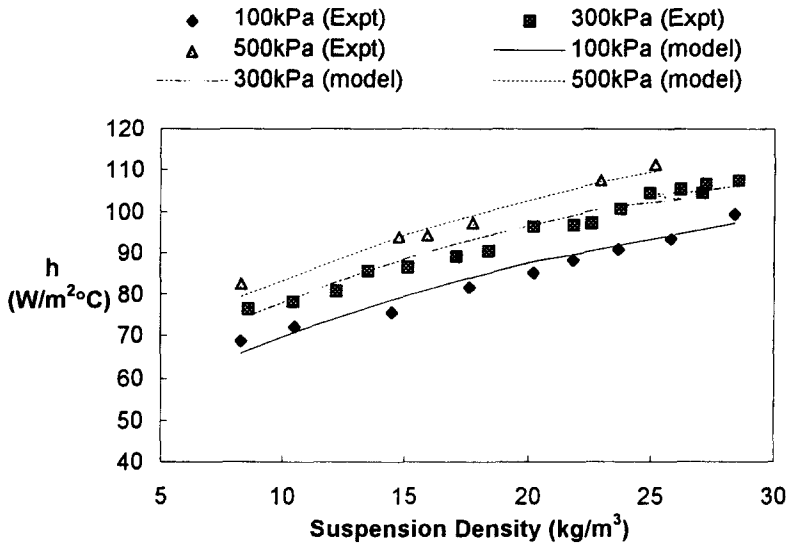

Fig. 6. Effect of suspension density on the heat transfer coefficients and comparison with the present model results (particle diameter: 0.507 mm).

more important role at higher pressures. Shen *et al.* [16] suggested that when the system pressure is high the contribution of the heat transfer due to the gas phase will also rise.

Effect of superficial gas velocity

To operate the bed under a pre-determined superficial gas velocity, the suspension density could be changed by adjusting the loop-seal control valve. Figure 7 shows the variation of the heat transfer coefficient with the suspension density at different superficial velocities and the model results. Experimental data in Fig. 7 show that the heat transfer coefficients at different superficial velocities are very close to each other. However, the situation may be different at high pressure and low suspension density. In such conditions the contribution of the gas phase will be more important and therefore, the effect of superficial gas velocity may become prominent.

Effect of particle size

The bed-to-wall heat transfer coefficient measured at 300 kPa for two particle sizes are plotted against suspension densities (Fig. 8). Finer particles give higher heat transfer coefficients. Shen *et al.* [16] also observed the same phenomenon. This feature is similar to that observed in atmospheric pressure CFBs having a short heat transfer section.

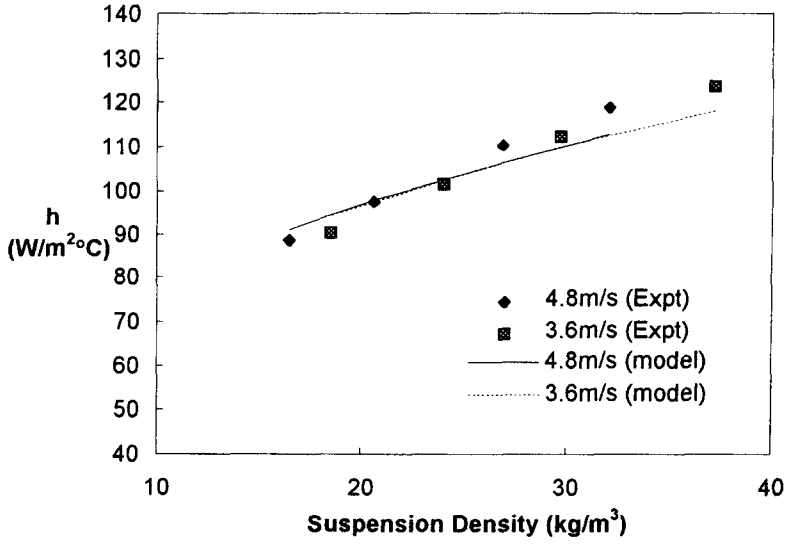

Fig. 7. Effect of superficial velocity on the heat transfer coefficients and comparison with the present model results (particle diameter: 0.507 mm).

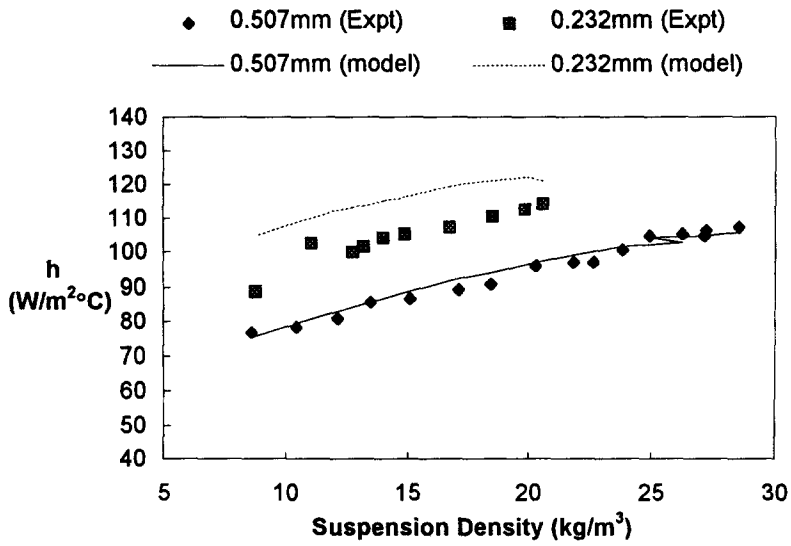

Fig. 8. Effect of particle size on the heat transfer coefficients and comparison with the present model results (system pressure: 300 kPa).

The above observation can be explained from equation (4). Smaller particles have lower contact resistance at the wall ($d_p/10K_{gf}$). However, a longer heat transfer section resulting in longer cluster residence time (t_c) may not experience the particle size effect because the second term in the denominator of equation (4) becomes dominant, and also because finer particles may result in lower cluster thermal conductivity [equation (5)]. The residence time may be influenced by the effect of pressure on particles' aggregation and motion in the bed.

The model results are also plotted on Fig. 8. The model's predictions did not artificially keep the velocity constant. It took note of slight variations in the velocity that occurred from one point to the other. For this reason the theoretical curve is not as smooth as one would expect had all other parameters, except the suspension density, been kept unchanged. The predictions agree well with the experimental data for a 0.507 mm particle. However, for a 0.232 mm particle, the model results are about 8% higher than the test data. Such errors in the prediction of the heat transfer coefficient are common. One can speculate that the cluster voidage from equation (2) may also be influenced by particle size. In the absence of further study no definite conclusion on this can be drawn.

Effect of bed temperature

Figure 9 plots the heat transfer coefficients, measured at 300 kPa, against bed suspension densities for two temperatures 750°C and 250°C. A higher bed temperature results in a higher heat transfer coefficient. It also shows a minimal effect of the superficial gas velocity. The observed rise in heat transfer coefficient with the bed temperature is attributed to the increase in thermal conductivity of the fluidizing gas and the increase in radiation from the bed at higher temperatures.

Dimensional analysis and empirical relation

The mechanistic model presents a good explanation of the effects of different parameters which is used for scale up purposes. However, its effectiveness for computation of the heat transfer coefficient for design is somewhat limited, owing to the lack of precise values of K in equation (1) and Y in equation (6). Also in the cluster residence time t_c, the maximum length over which a wall cluster maintains its identity, cannot be found easily. So an attempt was made to examine if an empirical relation can be developed based on dimensional analysis to correlate the present data and those others. However, caution must be applied in using such a correlation for PCFB units much larger than the present one.

Except for one equation (9) proposed by Shen *et al.* [16], no empirical correlation is available for the estimation of the heat transfer coefficient in a PCFB.

$$Nu_w = 1.06\times 10^7\left(\frac{1}{Re_p}\right)^{0.7294}\left(\frac{\rho_g}{\rho_0}\right)^{0.6772} \times\left(\frac{U_g}{U_t}\right)^{0.5111}(1-\varepsilon)^{0.2767}\left(\frac{d_p}{D}\right)^{2.1498}. \quad (9)$$

To correlate the present set of data a dimensional analysis was carried out. Eleven correlations with different combinations of dimensionless parameters such as $1-\varepsilon$, Reynolds number Re_p, ρ_g/ρ_0, d_p/D, C_p/C_g, Prandtl number Pr, U_g^2/gd_p and Archimedes number Ar, were attempted. Comparing their root mean square deviations and maximum relative devi-

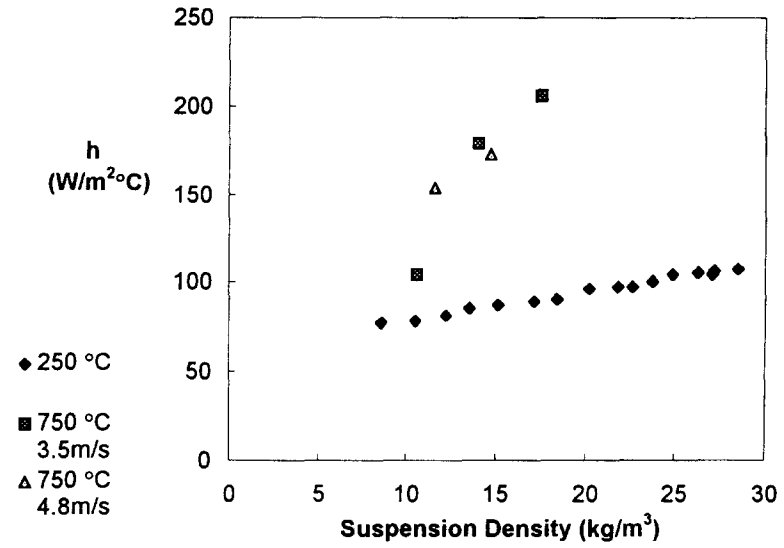

Fig. 9. Effect of bed temperature on heat transfer coefficients (system pressure: 300 kPa).

ations, equation (10) is proposed here for prediction of heat transfer coefficients. The data from present tests were substituted into equation (9) and (10), their root mean square deviations are 815.2 and 0.11, respectively. The maximum relative deviations are 451 and 10.9%, respectively.

$$Nu_w = 735\left(\frac{C_p}{C_g}\right)(1-\varepsilon)^{0.32}\left(\frac{\rho_g}{\rho_0}\right)^{0.11}\left(\frac{d_p}{D}\right)^{0.92} Pr. \tag{10}$$

Figure 10 shows the comparison of the results from equation (10) and the experimental data. The calculation results agree well with these test data.

Comparison with previous work

Only a few data were available on the heat transfer coefficient in a PCFB at the time of writing this paper. Shen *et al.* [16] carried out tests on a 6 m high and 80 mm ID tube PCFB cold test rig. The experimental data of Shen *et al.* [16] were first compared with the heat transfer coefficients predicted using the proposed model. Figure 11(a, b) shows the comparison of model predictions and their test results for two sizes of particles. A good agreement between the predicted results from the model with those of the experimental data of Shen *et al.* [16] is apparent on Fig. 11 (a, b).

Shen *et al.* [16] correlated their test data and proposed the equation (9). While they succeeded in correlating their own data, their correlation over predicted the present experimental results.

CONCLUSION

(1) The bed-to-wall convective heat transfer coefficient increases with increasing system pressures

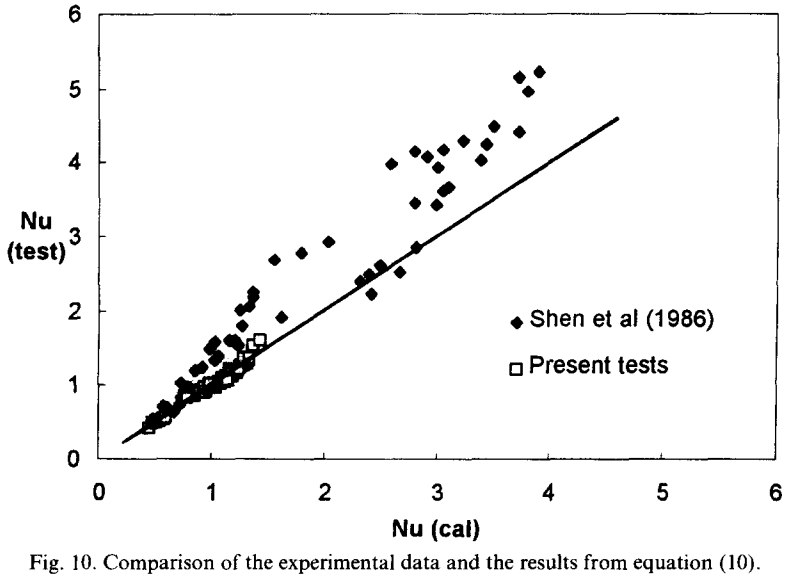

Fig. 10. Comparison of the experimental data and the results from equation (10).

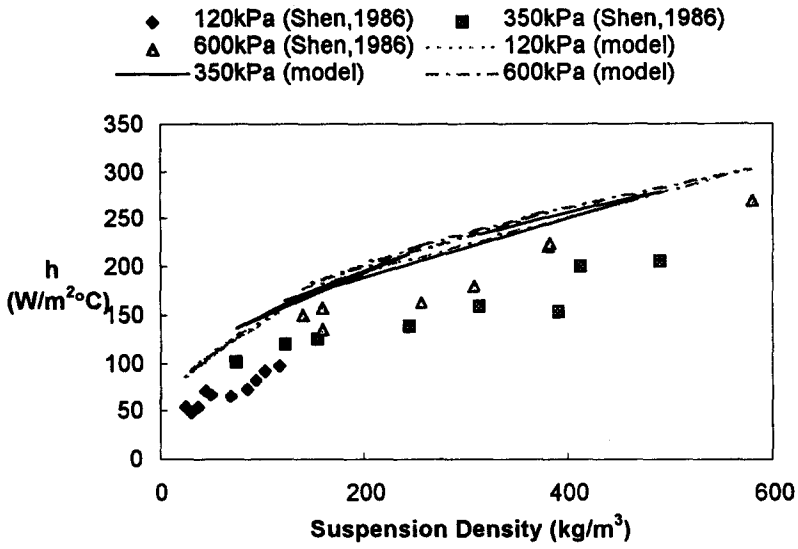

(a) particle size: 0.25mm

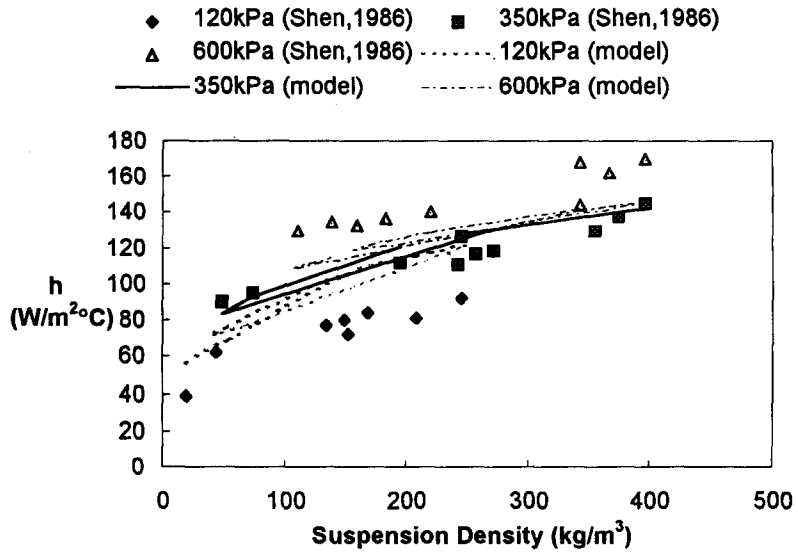

(b) particle size: 0.77mm

Fig. 11. Comparison of the model results with Shen *et al.* [16] test data, (a) particle size 0.25 mm, (b) particle size 0.77 mm.

and bed suspension density, but not with particle size for a short heat transfer surface. The effect of superficial gas velocity on the heat transfer coefficient is negligible.

(2) The effect of system pressure on the heat transfer coefficient can be explained by its effect on the gas density and cluster thermal conductivity. No major effect of the additional hydrodynamic changes was observed within the limited range of the present experiments.

(3) The modified cluster renewal model predicts the heat transfer coefficient with a reasonable accuracy.

(4) An empirical relation is proposed to predict the heat transfer coefficient at room temperature.

Acknowledgement—The authors acknowledge the financial support of the Canadian International Development Agency (CIDA). The authors also thank Mr Bill Bowness and Mr Jamie MacKay in building the test rig.

REFERENCES

1. Babcock and Wilcox, In *Steam/Its Generation and Use* (40th Edn) (Edited by S. C. Stultz and J. B. Kitto), Chap. 29. Babcock & Wilcox, OH (1992).
2. P. Basu, Heat transfer in high temperature fast fluidized beds, *Chem. Engng Sci.* **45,** 3123–3136 (1990).
3. P. Basu and S. A. Fraser, In *Circulating Fluidized Bed Boilers: Design and Operations*, Chap. 3. Butterworth-Heinemann, London (1991).
4. Y. Tung, J. Li and M. Kwauk, Radial voidage profile in a fast fluidized bed. In *Fluidization* 88 (Edited by M. Kwauk and D. Kunii), pp. 139–145. Science Press, Beijing, (1988).
5. M. Lints, Particle-to-wall heat transfer in circulating fluidized beds, Doctoral Thesis, Massachusetts Institute of Technology, Cambridge, MA (1992).
6. R. L. Wu, C. J. Lim and J. R. Grace, The measurement of instantaneous local particle transfer coefficient in a circulating fluidized bed, *Can. J. Chem. Engng* **67,** 301–307 (1989).
7. S. Dou, Experimental study of heat transfer in circulating fluidized beds, doctoral Thesis, Lehigh University, U.S.A. (1990).
8. M. Louge, J. Lischer and H. Chang, Measurement of voidage near the wall of a circulating fluidized bed riser, *Powder Technol.* **62,** 269–276 (1990).
9. A. M. Xavier and J. F. Davidson, Heat transfer in fluidized beds: convective heat transfer in fluidized beds. In *Fluidization* (2nd Edn) (Edited by J. F. Davidson, R. Clift and D. Harrison), pp. 443–450. Academic Press, London (1985).
10. D. Kunii and O. Levenspiel, *Fluidization Engineering* (2nd Edn). Butterworth-Heinemann, Stoneham (1991).
11. L. R. Gliskman, Circulating fluidized bed heat transfer. In *Circulating Fluidized Bed Technology II*, pp. 13–29. Pergamon Press, Oxford (1988).
12. H. Martin, The effect of pressure and temperature on heat transfer to gas-fluidized beds of solid particles. In *Heat and Mass Transfer in Fixed and Fluidized Beds* (Edited by W. P. M. van Swaaij and N. H. Afgan), pp. 143–157. Hemisphere, New York (1985).
13. C. Y. Wen and E. N. Miller, Heat transfer in solid-gas transport lines, *Ind. Engng Chem.* **53,** 51–53 (1961).
14. A. Haider and O. Levenspiel, Drag coefficient and terminal velocity of spherical and nonspherical particles, *Powder Technol.* **58,** 63–70 (1989).
15. R. H. Perry, and Don Green, *Perry's Chemical Engineers' Handbook* (6th Edn), pp. 3–162 (1984).
16. Shen Xianglin, Zhou Naijun and Xu Yiqian, Experimental study on heat transfer in a pressurized circulating fluidized bed. In *Circulating Fluidized Bed Technology III* (Edited by P. Barn, M. Honio and M. Hasatani), pp. 451–456. Pergamon Press, Oxford (1991).